

Measurement of Reverse Flow Generated at Cold Exit of Vortex Tube

Mohd Hazwan bin Yusof, Hiroshi Katanoda

Abstract—In order to clarify the structure of the cold flow discharged from the vortex tube (VT), the pressure of the cold flow was measured, and a simple flow visualization technique using a 0.75mm-diameter needle and an oily paint is made to study the reverse flow at the cold exit. It is clear that a negative pressure and positive pressure region exist at a certain pressure and cold fraction area, and that a reverse flow is observed in the negative pressure region.

Keywords—Flow visualization, Pressure measurement, Reverse flow, Vortex tube.

I. INTRODUCTION

THE vortex tube (VT) is a simple and useful device to obtain both cold and hot flows from a compressed gas at room temperature. It can produce a cold flow measuring around -30°C and a hot flow of up to around 130°C . There are a lot of advantages to VT, such as being light, small, with no moving parts, no need for maintenance, and an instant supply of cold flow. The VT has been used mainly as a cooling device, such as for electrical pieces, thermal sensors, controlling cabins, cutting tools and areas under thermal stresses [1].

In 1930's, George Ranque [2] was the first to discover the energy/temperature separation phenomenon. Later in 1947, Hilsch [3] performed an experiment to investigate the mechanism of the vortex tube. Since then, the vortex tube is also known as Ranque-Hilsch Vortex Tube (RHVT).

Fig. 1 shows the flow pattern and structure of VT. Compressed air enters a VT through single tangential nozzle, or multiple tangential nozzles, and produces a high-speed vortical flow in the vortex chamber. A part of the flow rotates alongside the tube wall towards the opposite end, and the flow exits as a hot flow. Another part of the flow, at the core is forced back towards the vortex chamber by a control valve, and exits as a cold flow from an exit (cold exit).

Until now, several theories have been proposed about the thermal separation mechanism inside the VT by several researchers [2]-[5]. From these theories, it is generally accepted that, the temperature reduction of the cold flow, is caused by an adiabatic expansion of a compressed gas. However, details concerning the physics of the cold flow generation, from the fluid dynamics view point still remain unclear. Several

numerical and experimental works had been done to investigate the geometrical optimization of the VT. U. Behera et al.[6] performed a CFD analysis and experimental investigation to optimize the geometry of VT. They reported that the optimum size of the cold exit is 58% of the diameter of the tube. S.U. Nimbalkar [7] performed similar experiments to determine the optimum size of the cold exit. He reported that the optimum diameter of the cold end orifice is 50% of the diameter of the tube, which is 8% smaller than the result of U. Behera et al.[6]. K. Chang et al. [8] investigated the effect of a divergent hot tube to the performance of the VT. They reported that the performance of the VT can be improved by using the divergent hot tube with a divergent angle not more than 6° , compared to a conventional cylindrical tube VT.

Several researchers had studied experimentally and numerically on the pressure inside VT [9], [10]. However, the pressure of the flow discharged from VT has not been studied. In this research, the pressure of the cold flow discharged from the cold exit was measured, and the structure of the cold flow is discussed.

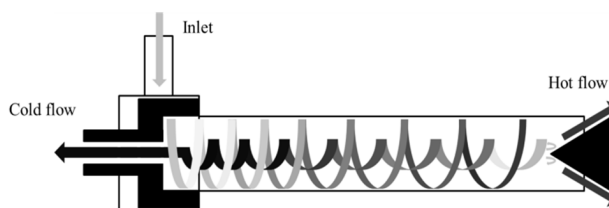


Fig. 1 Flow Pattern in Vortex Tube

II. EXPERIMENTAL SETUP

Fig. 2 shows a schematic diagram of the experimental setup of our VT. Compressed air up to 1MPa is supplied to the vortex chamber of the VT through (1) mass flow meters, (2) stagnation chamber and (3) pressure control valve. Then, a vortical flow is generated through the inlet tangential nozzles. The cold flow exit is located near the inlet tangential nozzles. The hot flow exit is at the opposite end of the tube. The inlet temperature, inlet pressure, cold flow temperature, and cold flow pressure were measured by a (4) temperature-humidity sensor, (5) total temperature probe, (6) digital manometer and (7) pressure sensor, respectively. The inlet pressures were varied in the range of 0.2~0.6MPa.

The geometry of the VT used in this research is shown in Fig. 3. It has an inner tube diameter of $D=14\text{mm}$ and a length to inner diameter ratio of $L/D=20$, a cold exit diameter of $d=5\text{mm}$, and four tangential nozzles.

Mohd Hazwan bin Yusof is with the Graduate School of Science and Engineering, Kagoshima University, 1-21-40, Korimoto, Kagoshima City, Kagoshima, 890-0065 Japan (phone: +81-99-285-8253; fax: +81-99-285-8253; e-mail: k1130849@kadai.jp).

H. Katanodais with the Graduate School of Science and Engineering, Kagoshima University, 1-21-40, Korimoto, Kagoshima City, Kagoshima, 890-0065 Japan (phone: +81-99-285-8250; fax: +81-99-285-8250; e-mail: katanoda@mech.kagoshima-u.ac.jp).

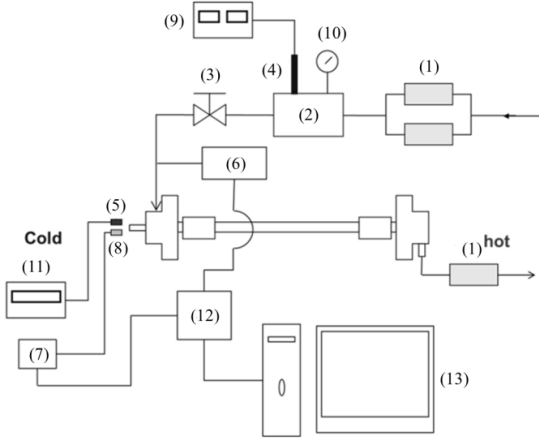


Fig. 2 Schematic diagram of the experimental setup. ((1)Mass flow meter, (2)Stagnation chamber,(3)Valve,(4)Temperature/humidity sensor,(5)Total temperature probe,(6)Digital manometer, (7)Pressure sensor, (8)Pitot pressure probe,(9)Temperature/humidity indicator,(10)Bourdon tube pressure gauge,(11)Temperature indicator, (12)AD conversion board, (13)Personal computer)

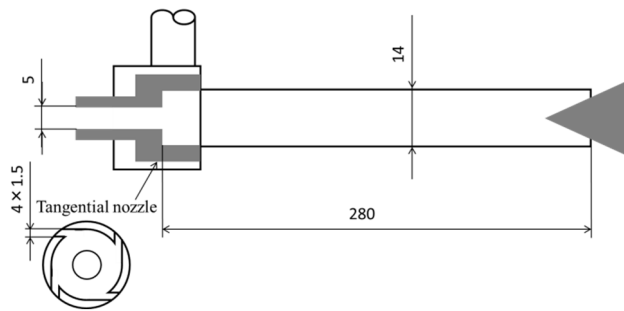


Fig. 3 Diameter of Vortex Tube

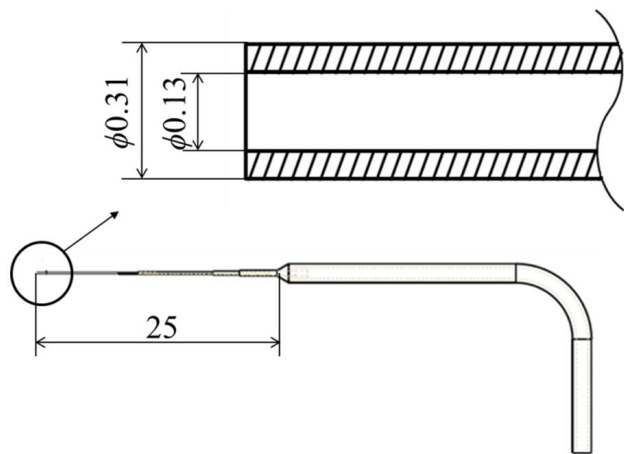


Fig. 4 Pitot pressure probe

Fig.5 shows the Pitot pressure probe used in this experiment. It has inner/outer diameters of 0.13/0.31mm, respectively. The pressures of the cold flow were measured

along the centerline of cold exit at a distance of 0 and 3mm from the exit ($x=0, 3\text{mm}$) using the Pitot pressure probe.

The ratio of the mass flow rate of cold flow, \dot{m}_{cold} , to the inlet mass flow rate, \dot{m}_{in} , is called cold fraction, which is defined as;

$$\varepsilon = \frac{\dot{m}_{cold}}{\dot{m}_{in}} \quad (1)$$

III. RESULTS AND DISCUSSION

A. Pressure Measurement

To understand the flow pattern at the cold exit, the pressure of the cold flow was measured by the Pitot pressure probe at $x=0, 3\text{mm}$ from the cold exit plane, along the center line. Figs. 5 (a) and (b) show a contour map of the measured Pitot pressure, divided by the atmospheric pressure, p_i/p_a , at $x=0, 3\text{mm}$, respectively. The horizontal axis shows the inlet pressure, p_{in} , and the vertical axis shows the cold fraction, ε . It can be seen from this figure that at a certain inlet pressure, when the cold fraction increases, the Pitot pressure inverts from negative ($p_i/p_a < 1.0$) to positive pressure ($p_i/p_a > 1.0$) at $x=0, 3\text{mm}$. The existence of p_i/p_a lower than 1.0 (negative pressure) implies the possible occurrence of a reversed flow around the center of the cold flow. This reversed flow will be discussed later. From Fig. 5 (a), the Pitot pressure in the region of $p_{in} > 0.45$ and $\varepsilon > 0.7$ is more than 2 times larger than atmospheric pressure. This implies the possibility of choking at the cold exit.

By comparing the data of the pressure measurement at $x=0$ and 3mm, the Pitot pressure at $x=3\text{mm}$ is smaller than the Pitot pressure at $x=0\text{mm}$ at a certain inlet pressure and cold fraction. To clarify the difference between the two contour maps, the Pitot pressure measured at $x=0\text{mm}$ is subtracted from that at $x=3\text{mm}$ and the result is shown in Fig. 6. As shown in this figure, the Pitot pressure differences are smaller than -0.2 for $p_{in} > 0.55$, $\varepsilon > 0.65$. This implies the possibility, of a choked under-expanded sonic jet, at the cold exit; the total pressure of the flow that passes through the shock wave generated at the probe tip is reduced.

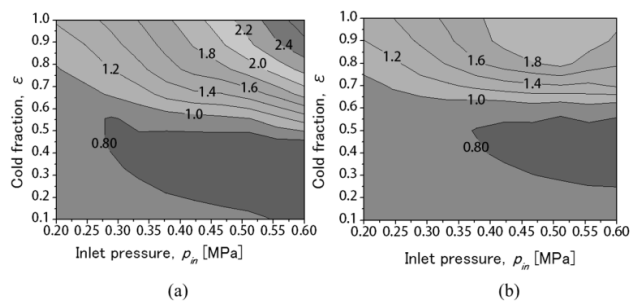


Fig. 5 Contour map of non-dimensionalized Pitot pressure, p_i/p_a at cold flow center; (a) $x=0\text{mm}$, (b) $x=3\text{mm}$

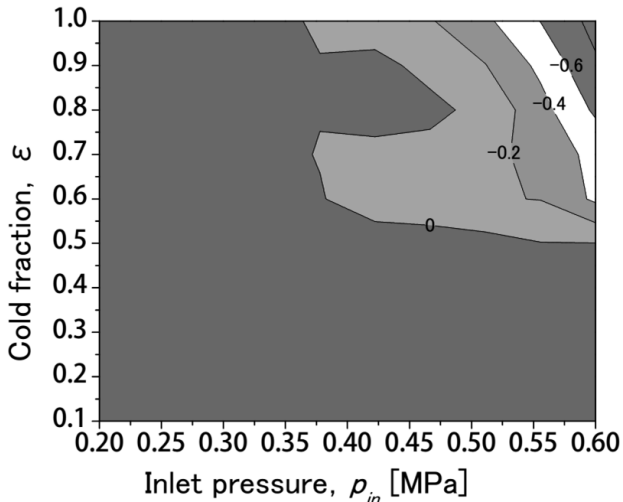


Fig. 6 Contour map of non-dimensionalized Pitot pressure differences between measurement of $x=0\text{mm}$ and 3mm

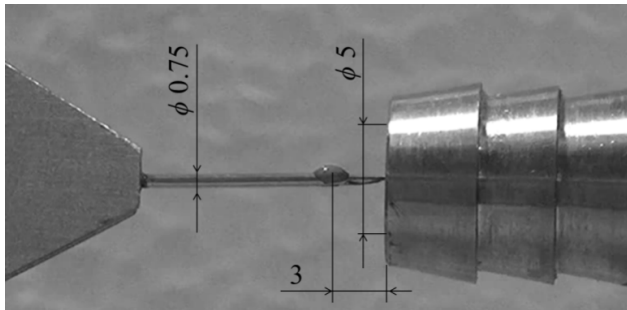


Fig. 7 Visualization setup for cold flow direction.

B. Visualization of Reverse Flow at Cold Exit

As discussed in Section 4, the existence of a negative pressure at the cold exit implies the possibility of a reverse flow at the cold exit. To verify this, a simple flow visualization technique is produced using a 0.75mm -diameter needle and an oily paint. Fig. 8 shows the flow visualization setup for observing cold flow direction. It can be seen from this figure that, a small amount of oil paint is dropped on a needle which was then inserted in the cold flow along the centerline. The distance of the oil paint center, and the cold exit, is fixed at $x=3\text{mm}$ which is equal to one of the distance of pressure measurements. The inlet pressures were varied from 0.2 to 0.6 MPa at 0.1 MPa intervals. For each inlet pressure, the cold fraction was varied from 0.1 to 0.9 to observe the flow, to determine the stagnation point and flow direction at $x=3\text{mm}$ from the cold exit plane.

Figs. 8 (a) and (b) show a visualization result at $p_{in}=0.2$ MPa and $\epsilon=0.33$, before and after the experiment, respectively. As shown in this figure, the oil paint moved towards the cold exit, indicating the existence of a reverse flow at $x=3\text{mm}$ from the cold exit. Figs. 9 (a) and (b) show a visualization result at $p_{in}=0.2\text{MPa}$ and $\epsilon=0.71$, before and after the experiment, respectively. It can be seen from these results that, the oil paint remained at $x=3\text{mm}$ which indicates a stagnation point in

the cold flow. This stagnation point is a boundary point for the reverse flow and the direct flow.

Figs. 10 (a) and (b) show a visualization result at $p_{in}=0.2\text{MPa}$ and $\epsilon=0.84$, before and after the experiment, respectively. As shown in this figure, the flow at $x=3\text{mm}$ was a direct flow. From Figs. 8 to 10, it can be concluded that a reverse flow exists at a certain cold fraction area and distance from the cold exit.

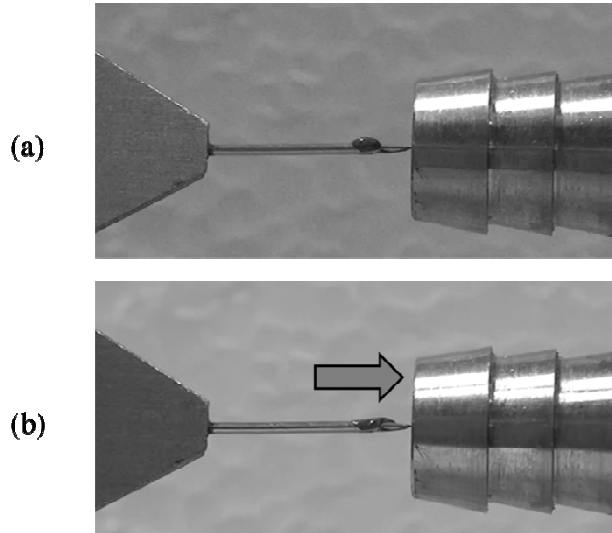


Fig. 8 Visualization result at $p_{in}=0.2\text{MPa}$, $\epsilon=0.33$; (a) before, (b) after

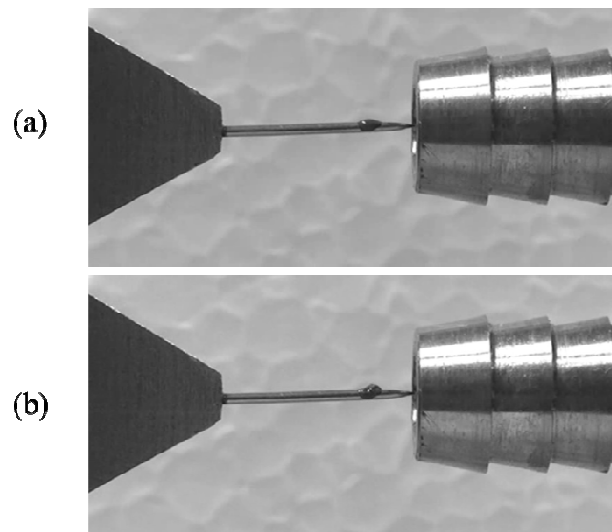


Fig. 9 Visualization result at $p_{in}=0.2\text{MPa}$, $\epsilon=0.71$; (a) before, (b) after

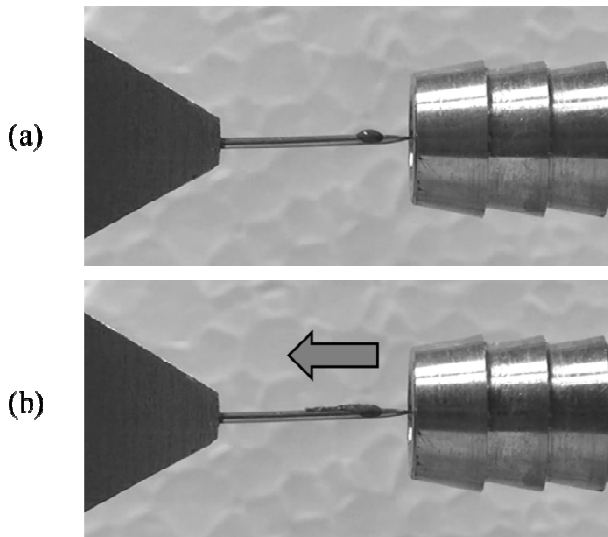


Fig. 10 Visualization result at $p_{in}=0.2\text{MPa}$, $\epsilon=0.84$; (a) before, (b) after

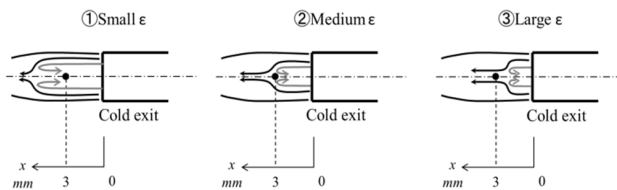


Fig. 11 Flow pattern at the cold exit of vortex tube

C.Flow Pattern of the Cold Flow at the Cold Exit

Fig. 11 shows the flow pattern at the cold exit of our vortex tube. For a small cold fraction area, the reverse flow region at the cold exit is large, which exceeded the pressure measurements distance from the cold exit. For a medium cold fraction, the reverse flow region shrinks and the stagnation point moves towards the cold exit. When the cold fraction increases, the reverse flow region decreases to less than 3mm from the cold exit. It can be concluded that the cold fraction point has the main role in controlling the size of the reverse flow at the cold exit.

IV. CONCLUSION

Experimental study of VT was conducted to measure the pressure of cold flow discharged from the VT. In addition, a simple flow visualization method was used to observe the reverse flow at the cold exit. The results obtained in this study are summarized as follows;

- 1) The Pitot pressure decreases when the Pitot pressure probe is traversed from $x=0\text{mm}$ to $x=3\text{mm}$, which shows the cold flow is an under expanded jet for $p_{in}>0.55$, $\epsilon>0.65$.
- 2) When the cold fraction increases, the Pitot pressure inverts from negative pressure to positive pressure for $x=0, 3\text{mm}$, and the flow inverts from reverse flow to direct flow for $x=3\text{mm}$ at a certain inlet pressure.

- 3) The inversion of reverse to direct flow occurs at a small cold fraction when the inlet pressure increases.

REFERENCES

- [1] S. Eiamsa-ard, P. Promvonge, Review of Ranque-Hilsch effects in vortex tubes. *Renew. Sustain. Energy Rev.*, vol. 12, pp. 1822-1842, 2008.
- [2] G. J. Ranque, Experiences sur la de 'tentegiratoire avec productions simultanees dun echappementdairchaudet dun echappementdairfroid. *J. Phys. Rad.*, vol. 7, no. 4, pp. 112-114, 1933.
- [3] R. Hilsch, The use of expansion of gases in a centrifugal field as cooling process, *Rev.Sci.Instrum.*, vol. 18, no. 2, pp. 108-113, Feb. 1947.
- [4] C.U. Linderstrom-Lang, The three-dimensional distributions of tangential velocity and total-temperature in vortex tubes, *J. Fluid Mech.*, vol. 45, pp. 161-187, Jan. 1971.
- [5] R.Z. Alimov, Flow friction and heat and mass transfer in a swirled flow, *J. Eng. Phys. Thermophys.*, vol. 10, no. 4, 251-257, 1966.
- [6] UpendraBehera et al., CFD analysis and experimental investigations towards optimizing the parameters of Ranque-Hilsch vortex tube, *Int. J. Heat Mass Transfer.*, vol. 48, pp. 1961-1973, May 2005
- [7] S.C. Nimbalkar, M.R. Muller, An experimental investigation of the optimum geometry for the cold end orifice of a vortex tube, *Appl. Therm. Eng.*, vol. 29, pp. 509-514, Feb. 2009.
- [8] Kun Chang et al., Experimental investigation of vortex tube refrigerator with a divergent hot tube, *Int.J.Refrigeration*, pp. 322-327, Jan. 2011.
- [9] Y. Xue, M. Arjomandi, R. Kelso, Experimental study of the flow structure in counter flow Ranque-Hilsch vortex tube, *Int. J. Heat Mass Transfer.*, vol. 55, pp. 5853-5860, Oct. 2012.
- [10] U. Behera, P.J. Paul, K. Dinesh, S. Jacob, Numerical investigations on flow behaviour and energy separation in Ranque-Hilsch vortex tube, *Int. J. Heat Mass Transfer.*, vol. 51, pp. 6077-6089, Dec. 2008.